

The ENUBET Project.

A high precision narrow-band neutrino beam

G. Brunetti*

INFN Sezione di Padova

E-mail: giulia.brunetti@pd.infn.it

F. Acerbi^a, G. Ballerini^{b,c}, M. Bonesini^c, A. Branca^{d,e}, C. Brizzolari^{c,f}, S. Capelli^{b,c}, S. Carturan^g, M.G. Catanesi^h, S. Cecchiniⁱ, N. Charitonidis^l, F. Cindoloⁱ, G. Collazuol^{d,e}, E. Conti^d, F. Dal Corso^d, C. Delogu^{d,e}, G. De Rosa^{m,n}, A. Falcone^{c,f}, B. Goddard^l, A. Gola^a, C. Jollet^{o,p}, V. Kain^l, B. Klicek^q, Y. Kudenko^r, M. Laveder^{d,e}, A. Longhin^{d,e}, L. Ludovici^s, E. Lutsenko^{b,c}, L. Magaletti^h, G. Mandrioliⁱ, A. Margotti^l, V. Mascagna^{b,c}, N. Mauriⁱ, L. Meazza^{c,f}, A. Meregaglia^p, M. Mezzetto^d, A. Paoloni^t, M. Pari^{d,e}, E. Parozzi^{c,f}, L. Pasqualini^{l,u}, G. Paternoster^a, L. Patriziiⁱ, M. Pozzatoⁱ, M. Prest^{b,c}, F. Pupilli^d, E. Radicioni^h, C. Riccio^{m,n}, A.C. Ruggieri^m, C. Scian^e, G. Sirriⁱ, M. Soldani^{b,c}, M. Stipcevic^q, M. Tentiⁱ, F. Terranova^{c,f}, M. Torti^{c,f}, E. Vallazza^c, F. Velotti^l, M. Vesco^g, L. Votano^t

^aFondazione Bruno Kessler (FBK) and INFN TIFPA, Trento, Italy; ^bPhys. Dep., Università degli studi dell'Insubria, Como, Italy; ^cINFN, Sezione di Milano-Bicocca, Milano, Italy; ^dINFN Sezione di Padova, Padova, Italy; ^ePhys. Dep. Università di Padova, Padova, Italy; ^fPhys. Dep. Università di Milano-Bicocca, Milano, Italy; ^gINFN Laboratori Nazionali di Legnaro, Legnaro (PD), Italy; ^hINFN Sezione di Bari, Bari, Italy; ⁱINFN, Sezione di Bologna, Bologna, Italy; ^lCERN, Geneva, Switzerland; ^mINFN, Sezione di Napoli, Napoli, Italy; ⁿPhys. Dep. Università degli Studi di Napoli Federico II, Napoli, Italy; ^oIPHC, Université de Strasbourg, CNRS/IN2P3, Strasbourg, France; ^pCENBG, Université de Bordeaux, CNRS/IN2P3, 33175 Gradignan, France; ^qCenter of Excellence for Advanced Materials and Sensing Devices, Ruder Boskovic Institute, Zagreb, Croatia; ^rInstitute of Nuclear Research of the Russian Academy of Science, Moscow, Russia; ^sINFN, Sezione di Roma 1, Rome, Italy; ^tINFN, Laboratori Nazionali di Frascati, Frascati (Rome), Italy; ^uPhys. Dep. Università di Bologna, Bologna, Italy

The knowledge of initial flux, energy and flavor of neutrino beams is currently the main limitation for a precise measurement of neutrino cross sections. The ENUBET project is studying a facility based on a narrow band neutrino beam capable of constraining the neutrino fluxes normalization through the monitoring of the associated charged leptons in an instrumented decay tunnel. In particular, the identification of large-angle positrons from K_{e3} decays at single particle level can potentially reduce the ν_e flux uncertainty at the level of 1%.

The ENUBET Collaboration presented at EPS-HEP2019 the advances in the design and simulation of the hadron beam line, the performance of positron tagger prototypes tested at CERN beamlines, a full simulation of the positron reconstruction chain and the expected physics reach.

*European Physical Society Conference on High Energy Physics - EPS-HEP2019 -
10-17 July, 2019
Ghent, Belgium*

*Speaker.

1. The ENUBET Project and the monitored neutrino beams

The ENUBET ERC project (2016-2021) is studying a narrow band neutrino beam where lepton production can be monitored at single particle level in an instrumented decay tunnel (the tagger). This would allow to measure ν_μ and ν_e cross sections at the GeV scale with a precision improved by about one order of magnitude compared to present results. Such an experimental input would be highly beneficial to reduce the budget of systematic uncertainties in the next long baseline oscillation projects. Neutrino cross sections play a crucial role in the oscillation physics of the next generation $\nu_\mu \rightarrow \nu_e$ experiments and are mainly limited by the estimate of the initial flux that relies on the simulation of the beam line and on the limited knowledge of the hadro-production in targets. ENUBET [1, 2] addresses this problem by developing a neutrino source based on tagging of large angle positrons from the three body semi-leptonic K_{e3} decays ($K^+ \rightarrow e^+ \pi^0 \nu_e$) in an instrumented decay tunnel.

2. The ENUBET hadron beamline

The ENUBET beamline will allow performing ν_μ cross section studies with a narrow band beam and ν_e cross section measurement with 1% precision. This can be achieved using conventional magnets by maximising the number of K^+ and π^+ at tunnel entrance, by minimising the total length of the transferline to reduce kaon decay losses and by keeping under control the level of transported background. Momentum and charge-selected hadrons being injected in the instrumented decay tunnel need to be collimated enough such that any undecayed meson is capable of escaping the region without hitting the tagger inner surface: it keeps the rate of particles in the instrumentation at an acceptable level and allows to monitor the large angle decay products of kaon decays. Furthermore it is very important to tune the shielding and the collimators to minimise any beam induced background in the decay region. The beamline presented here is composed by a short (~ 20 m) transferline followed by a 40 m long decay tunnel, the length of the decay tunnel is optimized in order to have $\sim 97\%$ of the overall ν_e flux from K_{e3} decays (the rest arising from muon decays).

The optimization of the optics is performed with TRANSPORT [7] using a reference momentum of 8.5 GeV/c and a momentum bite of 10% to match ENUBET specifications. Particle transport and interactions in the beamline are simulated with G4beamline [8]. A horn-based beamline employs a pulsed horn between the target and the transport line while in a static system the transport and focusing line is implemented directly after the target. The proton interactions in the target (POT, protons on target) are simulated with FLUKA and we have considered various proton drivers (400 GeV, 120 GeV and 30 GeV protons) and target designs. The results reported in this document refer to 400 GeV protons and a 110 cm long beryllium target with a 3 mm diameter.

Preliminary results obtained with the static option look very promising: by using a triplet-dipole-triplet scheme we obtain hadronic rates at the decay tunnel entrance that are 4 times better than the first estimate presented in [1]. In Tab. 1 are reported our expected fluxes at the tagger entrance.

2.1 The static transfer line

The static configuration is very appealing since it allows to perform the focusing using DC

Focusing	π^+ /POT [10^{-3}]	K^+ /POT [10^{-3}]	Extraction Length	Factor w.r.t. [1]
Horn-based	77	7.9	2 ms	$\times 2$
Static	19	1.4	2 s	$\times 4$

Table 1: Expected rates of π^+ and K^+ in [6.5, 10.5] GeV/c range at the decay tunnel entrance for the two possible focusing schemes. The improvement factor in kaon transport with respect to [1] is shown in the last column.

operated devices (unlike pulsed magnetic horns) compatible with a traditional slow extraction of several seconds reducing pile-up effects and particle rates, thus opening the possibility to directly monitor the rate of muons from π^+ decays after the hadron dump so that the ν_μ flux could be monitored with the same level of precision of ν_e .

The ENUBET beam is a conventional narrow band beam, the best configuration achieved consists in a quadrupole triplet followed by a dipole that provides a 7.4° bending angle and by another quadrupole triplet (see Fig. 1). Off-momentum particles reaching the decay tunnel are mostly low energy particles coming from interactions in the collimators and other beamline components together with muons that cross absorbers and collimators. At 8.5 GeV/c we expect $\sim 50\%$ of K^+ to decay in a 40 m long tunnel. The rate of background particles is several orders of magnitude smaller than present beams and the instrumentation located in the decay tunnel can monitor lepton production at single particle level. Fig. 2 shows the momentum distribution as well as the profile in the plane perpendicular to the beam axis (XY) of K^+ entering/exiting the decay tunnel.

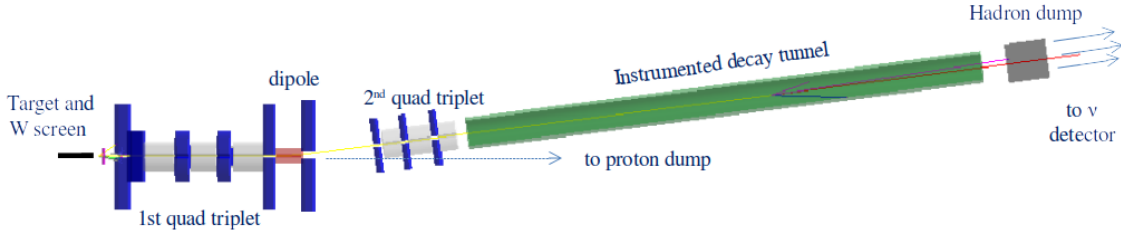


Figure 1: Schematics of the static line design.

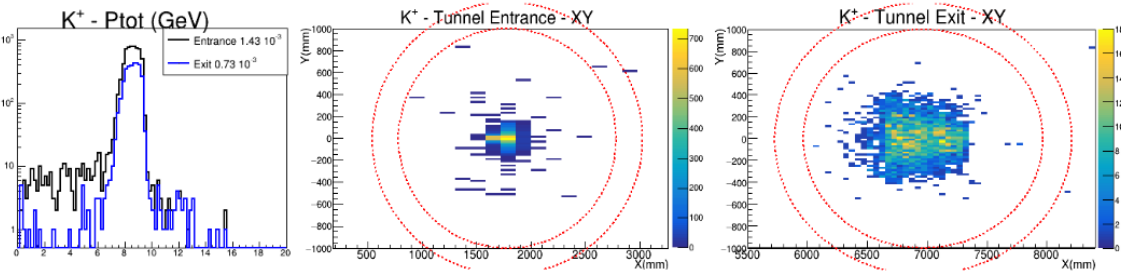


Figure 2: Left: momentum distribution of K^+ entering/exiting the decay tunnel. Right: XY profile of the K^+ beam at tunnel entrance and exit.

The static beamline transports at the tunnel entrance 19×10^{-3} π^+ /POT and 1.4×10^{-3} K^+ /POT in [6.5, 10.5] GeV/c range. This corresponds to about 4.5×10^{19} POT at CERN SPS to carry out both ν_μ and ν_e cross section programs.

Additional static focusing options are under study, by putting all inputs together we try to pin down the best design in terms of physics and technical feasibility. A 2-dipoles scheme is being investigated to improve the quality of the beam in the tagger: the larger bending angle (15.1°) would reduce the background from muons and it would be less probable for neutrinos produced in the beamline section collinear with the proton target to reach the neutrino detector.

2.2 The horn-based transfer line

In the horn-based solution a magnetic horn is placed between the target and the following transferline. Though the horn-based solution would provide higher yields at the decay tunnel one has to consider the horn pulse limit and the tagger rate limit that would be reached with $\sim 10^{12}$ POT per spill. The studies concerning the proton extraction scheme (“burst-mode extraction”) to combine a few ms proton extraction with 2-10 ms horn pulses are on-going at CERN. Burst mode operation has been demonstrated at the SPS in 2018 with 20 ms bursts. Feed forward burst optimization allows to further reduce the burst down to 10 ms, as shown in Fig. 3: the “AutospillBurst” algorithm developed leads to a burst length optimization from 20 to 10.6 ms. From this benchmark the studies will continue to explore the full simulation and to address remaining issues towards the full operability. The flux produced at the tunnel entrance is 4-5 times larger than in the static option: at the SPS we expect $77 \times 10^{-3} \pi^+/\text{POT}$ and $7.9 \times 10^{-3} K^+/\text{POT}$ in [6.5, 10.5] GeV/c range.

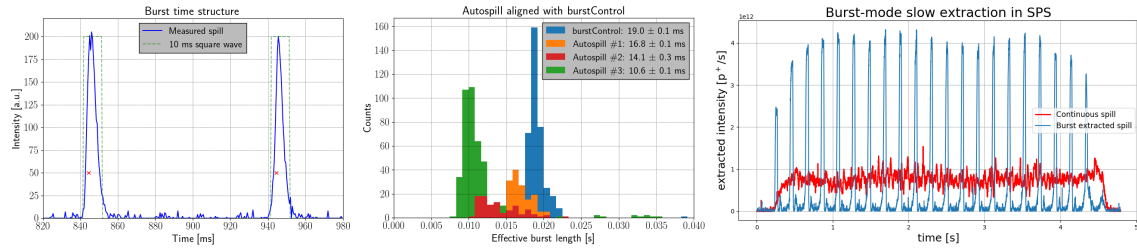


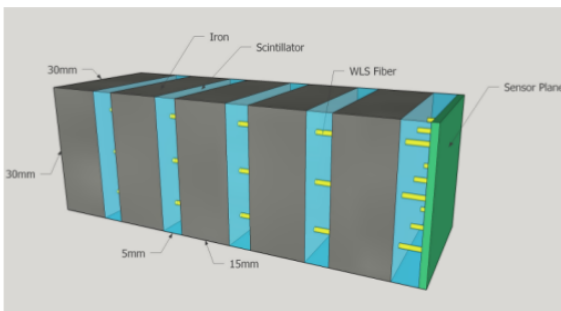
Figure 3: Left: algorithm of feed-forward implemented and capable of optimizing the burst length towards 10 ms. Center: the algorithm is capable to reduce the burst length from ~ 20 ms to 10.6 ms in 3 interactions. Right: burst extraction over a whole SPS spill performed during the ENUBET Machine Development study at CERN SPS in fall 2018 [9].

3. The positron tagger and detector R&D

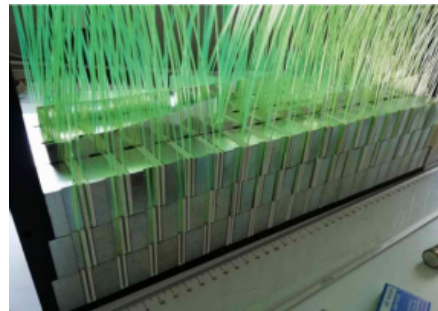
In the present ENUBET configuration the decay tunnel to be instrumented consists in an hollow cylinder with a length of 40 m and a 1 m radius. The maximum expected rate at the positron tagger is about 200 kHz/cm² and e/π separation better than 3% is needed to reject the pion background due to beam halo and to other kaon decay modes. This separation is achieved by means of longitudinally segmented calorimeters. The positrons from three body decays are emitted at large angles and hit the instrumented walls of the decay tunnel before exiting. Photons produced by π^0 decays are vetoed by plastic scintillator pads located just below the calorimeter. The photon veto also provides a precise timing of the positrons. These requirements constrain the detector technology, that must be based on radiation hard components with O(10 ns) recovery time and 10 cm² granularity. The reference design of the positron tagger is based on shashlik calorimetric

units (UCM) made of five, 15 mm thick, iron layers, interleaved with 5 mm thick plastic scintillator tiles (see Fig. 4a). The total thickness of the UCM module (10 cm) corresponds to $4.3 X_0$ and its transverse size is $3 \times 3 \text{ cm}^2$ providing e/π separation. The readout is performed in shashlik mode through 9 wavelength shifting fibers coupled to silicon photomultipliers (SiPM). The photon veto (that provides e^+/π^0 separation) is made of doublets of 5 mm thick plastic scintillator pads with a surface of $3 \times 3 \text{ cm}^2$, separated by a distance of 5 mm.

Different light readout options have been investigated and are discussed in the following section. The readout technology to be used will be decided after completing the analyses of the test beam data. The demonstrator prototype of the tagger is due by 2021, it will be 3 m long to allow the containment of shallow angle particles in realistic conditions and will cover a fraction of the total ϕ angle.



(a) Scheme of the baseline UCM.



(b) Lateral scintillation light readout.

3.1 Test beams of the calorimeter prototypes

A positron tagger prototype has been tested assembling 56 shashlik UCMs in a $7 \times 4 \times 2$ structure: 7 UCMs sample the development of the electromagnetic and hadronic showers in the longitudinal direction. This calorimeter was exposed at CERN-PS T9 beamline in November 2016 to a beam composed by electrons, muons and pions with momentum in the energy range of interest ([1, 5] GeV) in order to assess its performance [4].

In 2018 a different solution for the scintillation light readout was studied (see Fig. 4b). Light collected from scintillator sides are bundled to a single SiPM reading 10 fibers (1 UCM). Though less compact, in this layout SiPMs are not exposed to hadronic showers, neutron damage is reduced and it allows better accessibility for maintenance or replacements and better reproducibility of WLS-SiPM optical coupling. A prototype made of $3 \times 2 \times 2$ UCMs was assembled with each UCM composed by 1.5 cm thick iron slabs interleaved with 0.5 cm plastic scintillators (EJ-204), providing the same sampling term as the shashlik calorimeter. This prototype was tested at CERN-PS T9 beamline in May 2018. Another test beam was carried out in September 2018 with a larger prototype for better hadronic shower containment, consisting of a $7 \times 4 \times 3$ structure and integrating also the t_0 layer. The analysis of these data is still in progress but preliminary results show an electromagnetic energy resolution at 1 GeV of about 17%, consistent with the 15% prediction from a Monte Carlo simulation that does not include photon generation and transport. Moreover by placing 30 cm of borated polyethylene in front of the SiPMs a full FLUKA simulation considering 400 GeV protons shows an average neutron reduction factor of ~ 18 over the whole spectrum and even larger below 100 MeV.

3.2 Neutron irradiation test and the photon veto

During the lifetime of the experiment the SiPMs will integrate a neutron fluence of 1.8×10^{11} 1 MeV-equivalent neutrons/cm². A dedicated irradiation campaign was performed in 2017 using 3 PCBs hosting 9 SiPMs at the CN accelerator of the INFN-LNL laboratories. Each PCB integrated neutron fluences up to 10^{12} n/cm². In October 2017 UCM prototypes with larger scintillator thickness compared to the reference design and read out by the neutron irradiated SiPM boards were then tested at the CERN-PS T9 beamline. The tests [3] showed that the mip peak remains separated from the dark noise peak, the electron and mip peak mean value ratio is constant and the integrated neutron fluence does not affect the dynamic range of the photosensors. Hence, saturation effects due to the reduction of working pixels after irradiation are not visible at $O(10^{11}$ n/cm²).

During the tests at CERN (2016-2018) we were also able to perform the measurement of the photon-veto time resolution and we validated the 1-mip/2-mip separation capability using photon conversion from π^0 gammas. For SiPMs with a $3 \times 3 \times 0.5$ cm³ scintillator and 40 cm of WLS the light collection efficiency is $> 95\%$ and the time resolution is $\sigma_t \sim 400$ ps.

4. The ENUBET narrow-band beam

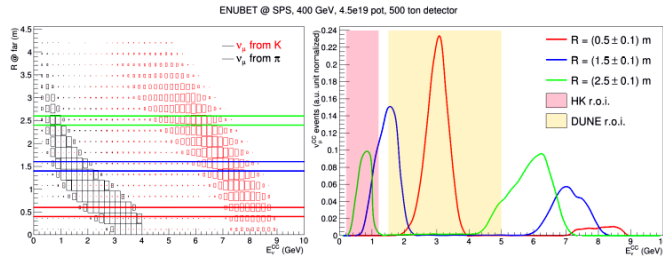
A full Geant4 simulation of the detector, from the transferline to the tagger, provides particle propagation and decays, the detector response at the hit level and pile-up effects. The analysis chain starts from the Event Builder that identifies the seed of the event, *i.e.* the UCM with largest energy deposit (> 20 MeV) in the inner layer. Then, neighboring cells close in time are clustered. The $e/\pi/\mu$ separation is performed with a multivariate TMVA analysis based on 6 variables (describing the pattern of energy deposition in the calorimeters). The signal on tiles of the photon veto (0-1-2 mip) is used for e/γ separation.

Assuming 4.5×10^{19} POT at the CERN-SPS, we expect to observe about 1.13×10^6 ν_μ^{CC} and 1.4×10^4 ν_e^{CC} interactions at a neutrino detector (500 t fiducial mass) located 50 m from the end of the tunnel. Thanks to the narrow band beam ν_μ from kaons and pions are well separated in energy. The tagger measurement constraints ν_e (K_{e3} decays) and ν_μ (mainly $K_{\mu 2}$ decays) from kaons.

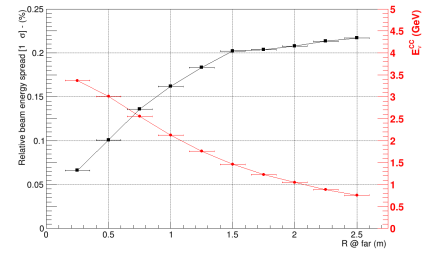
A narrow band beam such as ENUBET not only provides a beam with a precisely measured flux but also a measurement of the neutrino energy that does not rely on the reconstruction of final state particles (“narrow-band off-axis technique”). The static transfer line option has opened the possibility, now under study, of measuring the ν_μ from pions by placing a muon detector downstream the hadron dump at the decay tunnel exit. For ν_μ^{CC} interactions in the neutrino detector the neutrino energy is a function of the distance of the neutrino vertex from the beam axis (R) (see Fig. 5a). The incoming neutrino energy can be determined with a precision given by the pion peak width of the spectrum at a fixed R. It ranges from 8% for $R \sim 50$ cm at $\langle E_\nu \rangle \sim 3.5$ GeV to 22% for $R \sim 250$ cm at $\langle E_\nu \rangle \sim 0.7$ GeV (see Fig. 5b). The beam width at different fixed radius bins allows exploring the energy domain of DUNE/HK and would enrich samples of specific processes (QE, RES, DIS) for cross-section measurements.

4.1 Time tagged neutrino beams

A “tagged neutrino beam” is a facility where the neutrino is uniquely associated with the other particles of the parent kaon on an event-by-event base by tagging coincidences between ν_e at a



(a) Neutrino energy and ν_{μ}^{CC} events at the ENUBET neutrino detector as a function of the distance of the neutrino vertex from the beam axis (R).



(b) Energy resolution (black) and mean neutrino energy (red) as a function of R .

far detector and e^+ at the tagger. A scheme with a static focusing transferline with slow proton extraction lasting up to several seconds is mandatory since the instantaneous rates of particles hitting the decay tunnel walls is reduced by about two orders of magnitude compared with the horn option. At present with 2.5×10^{13} POT/s slow extraction one expects 1 genuine K_{e3} candidate every ~ 12 ns (80 MHz) with two times more background candidates (1 every ~ 4 ns). We need the time coincidence between the e^+ and the ν_e^{CC} interactions to be $|\delta t - \Delta/c| < \sigma_t$ where Δ is the distance between the e^+ and the ν_e interaction points and σ_t the combined time resolution for the positron tagger and the neutrino detector. A neutrino interaction in the detector time linked with the observation of its associated lepton in the decay tunnel has never been performed in any neutrino experiment and would represent a major breakthrough in experimental neutrino physics. This possibility is under study in the framework of ENUBET and the satellite NuTech Project funded by MIUR.

Acknowledgments

This project has received funding from the European Research Council (ERC) under the European Unions Horizon 2020 research and innovation programme (grant agreement N. 681647).

References

- [1] A. Longhin, L. Ludovici, F. Terranova, Eur. Phys. J. C **75** (2015) 155
- [2] A. Berra *et al.*, CERN-SPSC-2016-036, SPSC-EOI-014, Geneva, 2014.
- [3] F. Acerbi *et al.*, JINST **14** (2019) P02029.
- [4] G. Ballerini *et al.*, JINST **13** (2018) P01028.
- [5] A. Berra *et al.*, Nucl. Instrum. Meth. A **830** (2016) 345.
- [6] A. Berra *et al.*, IEEE Trans. Nucl. Sci. **64** (2017) 1056.
- [7] K. L. Brown *et al.*, TRANSPORT, A Computer Program for Designing Charged Particle Beam Transport Systems, 1983, CERN-80-04
- [8] T. J. Roberts and D. M. Kaplan, G4beamline simulation program for matter-dominated beamlines, 2007 IEEE Particle Accelerator Conference (PAC), Albuquerque, NM, (2007) 3468-3470
- [9] M. Pari, M. Fraser, B. Goddard, V. Kain, L. Stoel and F. Velotti, doi:10.18429/JACoW-IPAC2019-WEPMP035.